DETECTING STATIONARY PHASE POINTS IN THE TIME-FREQUENCY PLANE

Bernard Mulgrew (B.Mulgrew@ed.ac.uk)

School of Engineering, The University of Edinburgh, EH9 3JL, UK.

ABSTRACT

This paper describes and supplements a recent re-examination of linear time-frequency decomposition wherein the principle of stationary phase is applied to the synthesis integral. An inherent part of this time-frequency stationary phase approximation (TFSPA) is a test for the stationary phase condition itself. After outlining the development of the TFSPA, the main contribution of this paper is an analysis of the test from the perspective of classical detection theory. This leads to closed form approximations that; (i) quantify performance in terms of false alarm and detection probabilities; (ii) enable the development of improved tests.

Index Terms— cochlear filters; stationary phase approximation; ratio of complex Gaussian random variables.

1. INTRODUCTION

The paper contributes to a recent re-examination [1] of linear time-frequency (TF) decomposition [2]. The motivation is the resurgence of interest in analogue filter banks both as part of a synthetic cochlea and as a means to provide power efficient implementations of analysis filter banks [3]. The desire with both is to extract salient features from the TF decomposition using the limited functionality associated with analogue circuitry. The approach in [1] is to apply the principle of stationary phase (PSP) [4] to the TF synthesis integral through a new interpretation of the location parameters. The PSP had previously been applied to linear TF decomposition for both analysis, [5] & [6], and synthesis [7], the latter leading to the method of reassignment. The approach in [1] is to revisit [7] and to fundamentally re-interpret it. There is no attempt to either reassign [7] or relocate [8] components in the TF plane because of the limited functionality mentioned above.

Necessary definitions and background material are provided in Section 2. Section 3 outlines the TF stationary phase approximation (TFSA) introduced in [1] and, in particular, gives the test for stationary phase points based on the time-derivative and frequency-derivative filters associated with reassignment [7]. The main contribution of this paper is Section 4, where this test is analysed from the perspective of classical detection theory to quantify its performance and develop improved tests.

2. PRELIMINARIES

Consider a time-frequency analysis $X_\omega(t)$ of a signal of interest $x(t)$ of the form:

$$X_\omega(t) = x(t) * h_\omega(t), \;\; \{\omega : \omega_{min} < \omega < \omega_{max}\} \qquad (1)$$

where $*$ denotes convolution and the impulse response of a single filter in the analysis filter bank is $h_\omega(t) = \beta h(\beta t)\mathrm{e}^{\jmath\omega t}$. Each filter is formed using a prototype filter $h(t)$ and a bandwidth β that is itself a function of the centre frequency ω. The frequency response of the analysis filter is related to the frequency response of the prototype in a straight forward way, i.e. $H_\omega(\Omega) = \mathsf{F}[h_\omega(t)] = H\left(\frac{\Omega-\omega}{\beta}\right)$. where $H(\Omega) = \mathsf{F}[h(t)] = \int_{-\infty}^{\infty} h(t)\mathrm{e}^{-\jmath\Omega t}\,\mathrm{d}t$. While the Gaussian pulse is a common [2] and analytically convenient choice for time-frequency analysis, the gamma tone [9] and gamma chirp pulses [10] more closely model the cochlea in the ear. Details of these standard prototype filters and their properties are summarized in [1]. The prototype filters are normalised such that $H(0) = 1$. A re-synthesis, $\hat{x}(t)$, of the signal of interest is performed using filters matched to $h_\omega(t)$. Thus for real signals

$$\hat{x}(t) \;\; = \;\; \frac{1}{C}\Re\left\{\int_0^1\int_{-\infty}^{\infty} Z(\tau,\mu)\,\mathrm{d}\tau\mathrm{d}\mu\right\} \qquad (2)$$

with integrand $Z(\tau,\mu) \triangleq X_\omega(\tau)h_\omega^*(\tau - t)$ and where C is a constant. The time variable t is suppressed in this definition of the integrand to emphasize that the integration is respect to τ and the filter bank variable μ. The latter lies in the the range $[0,\,1]$ and is a monotonic function of ω. It provides a convenient way of dealing with a number of possible filter bank spacings. A value $\mu = 0$ indicates the lower edge of the filter bank and $\mu = 1$ indicates the upper edge. The bandwidth of the filter β is proportional to the derivative $\frac{\mathrm{d}\omega}{\mathrm{d}\mu}$, i.e. $\beta \propto \frac{\mathrm{d}\omega}{\mathrm{d}\mu}$. In the following ω_{min} is nominally the lowest frequency covered by the filter bank and ω_{max} is the maximum.

This work was supported by the Royal Academy of Engineering, SELEX ES and UK EPSRC

3. TF STATIONARY PHASE APPROXIMATION

Following [1], it is convenient to define normalized time- and frequency- derivatives of the integrand $Z(\tau,\mu)$, i.e. $Z_\tau \triangleq \frac{\frac{\partial}{\partial\tau}Z(\tau,\mu)}{Z(\tau,\mu)}$ and $Z_\mu \triangleq \frac{\frac{\partial}{\partial\omega}Z(\tau,\mu)\frac{d\omega}{d\mu}}{Z(\tau,\mu)}$ respectively, where

$$Z_\tau \quad = \quad \frac{\frac{\partial}{\partial\tau}X_\omega(\tau)}{X_\omega(\tau)} + \beta\frac{\dot{h}^*(\beta\{\tau-t\})}{h^*(\beta\{\tau-t\})} - \jmath\omega \qquad (3)$$

and

$$Z_\mu \quad = \quad \left\{\frac{\frac{\partial}{\partial\omega}X_\omega(\tau)}{X_\omega(\tau)} + \frac{\frac{\partial}{\partial\omega}h^*_\omega(\tau-t)}{h^*_\omega(\tau-t)}\right\}\frac{\mathrm{d}\omega}{\mathrm{d}\mu} \qquad (4)$$

where

$$\frac{\frac{\partial}{\partial\omega}h^*_\omega(\tau-t)}{h^*_\omega(\tau-t)} = \frac{\mathrm{d}\beta}{\mathrm{d}\omega}\left\{\frac{1}{\beta} + \frac{\dot{h}^*(\beta\{\tau-t\})}{h^*(\beta\{\tau-t\})}\{\tau-t\}\right\} - \jmath\{\tau-t\}$$

where $\dot{h}(t) = \frac{\mathrm{d}}{\mathrm{d}t}h(t)$. Both Z_τ and Z_μ are additions of a signal dependent term, e.g. $\frac{\frac{\partial}{\partial\tau}X_\omega(\tau)}{X_\omega(\tau)}$, and a signal independent term, e.g. $\frac{\frac{\partial}{\partial\tau}h^*_\omega(\tau-t)}{h^*_\omega(\tau-t)}$. The former is a function of the pair (ω,τ) whereas the latter is a function of the pair $(\omega,\tau-t)$. Note that $(\omega,\tau-t)$ are themselves parameters of the filter, specifically, the frequency where the filter has maximum gain ω and the delay $\tau-t$ between the input and output of the filter. In contrast to the method of re-assignment derived in [7], the delay term $\{\tau-t\}$ is interpreted as the group delay

$$\{\tau-t\} = g(\omega) \quad \triangleq \quad -\tfrac{\mathrm{d}}{\mathrm{d}\Omega}\angle H_\omega(\Omega)\big|_{\Omega=\omega} \qquad (5)$$

of the analysis filter at ω, where the notation $\angle H$ indicates the argument of the complex variable H. Thus (3) and (4) can be written as

$$Z_\tau \quad = \quad \frac{\frac{\partial}{\partial\tau}X_\omega(\tau)}{X_\omega(\tau)} + \beta\eta(\omega) - \jmath\omega \qquad (6)$$

and

$$Z_\mu = \left\{\frac{\frac{\partial}{\partial\omega}X_\omega(\tau)}{X_\omega(\tau)} + \frac{\mathrm{d}\beta}{\mathrm{d}\omega}\left\{\frac{1}{\beta} + \eta(\omega)g(\omega)\right\} - \jmath g(\omega)\right\}\frac{\mathrm{d}\omega}{\mathrm{d}\mu} \qquad (7)$$

respectively, where $\eta(\omega) = \frac{\dot{h}^*(\beta\{g(\omega)\})}{h^*(\beta\{g(\omega)\})}$. Then because $\Im\{\eta(\omega)\} = 0$ for all three filter types, the time derivative of the phase of the integrand is

$$Z_{\tau i} \quad = \quad \Im\{Z_\tau\} = \Im\left\{\frac{\frac{\partial}{\partial\tau}X_\omega(\tau)}{X_\omega(\tau)}\right\} - \omega \qquad (8)$$

and the frequency derivative is

$$Z_{\mu i} \quad = \quad \Im\{Z_\mu\} = \left\{\Im\left\{\frac{\frac{\partial}{\partial\omega}X_\omega(\tau)}{X_\omega(\tau)}\right\} - g(\omega)\right\}\frac{\mathrm{d}\omega}{\mathrm{d}\mu} \qquad (9)$$

Time and frequency derivatives of the analysis integral (1) are constructed using either the analysis filterbank itself as in [7] or from the derivative filters $\frac{\partial}{\partial\tau}h_\omega(\tau)$ and $\frac{\partial}{\partial\omega}h_\omega(\tau)$ respectively, c.f. [11]. Stationary phase points $\{(\omega_i,\tau_i)\}_i$ are solutions to $Z_{\tau i} = Z_{\mu i} = 0$. Locating stationary phase point requires a grid search over ω for a bank of analogue filters or over both ω and τ, for a discrete-time filter bank. Such a grid search is not onerous since it is implicit in the implementation of the analysis integral. With a grid search there is always the risk of missing a pair (ω_i,τ_i). This risk can be reduced by: (i) defining a phase gradient vector

$$\boldsymbol{\phi}(\tau,\mu) \quad \triangleq \quad [Z_{\tau i}\ \ Z_{\mu i}]^T \qquad (10)$$

where the superscript T indicates matrix transpose; (ii) using the Euclidean norm of this vector to construct a test for stationary phase points, i.e.

$$\|\boldsymbol{\phi}(\tau,\mu)\| \quad < \quad C_1 \qquad (11)$$

where the threshold C_1 is a small positive real constant. The Euclidean norm is used in [1] for analytic convenience when dealing with deterministic signals.

In addition to finding stationary phase points, equations (6) and (7) can also be used to test for phase-rate dominance in the TF plane [1]. For phase-rate dominance the inequality

$$\frac{p(\tau,\mu)}{\|\mathbf{a}(\tau,\mu)\|} \quad > \quad C_2 \qquad (12)$$

must be satisfied, where the amplitude gradient vector is $\mathbf{a}(\tau,\mu) \triangleq [\Re\{Z_\tau\}\ \ \Re\{Z_\mu\}]^T$ and the threshold C_2 is a positive real constant greater than or equal to one. The projection term

$$p(\tau,\mu) \quad = \quad \frac{|\boldsymbol{\phi}^T(\tau,\mu)\mathbf{W}\,\mathbf{a}(\tau,\mu)|}{\|\mathbf{a}(\tau,\mu)\|} \qquad (13)$$

is formed from the sum of the projection of the phase rate vector in the direction of the normalised amplitude rate, i.e. $\boldsymbol{\phi}^T\mathbf{a}/\|\mathbf{a}\|$, plus the projection in the orthogonal direction, i.e. $\boldsymbol{\phi}^T\left[\begin{smallmatrix}0 & 1\\ -1 & 0\end{smallmatrix}\right]\mathbf{a}/\|\mathbf{a}\|$ and hence $\mathbf{W} = \left[\begin{smallmatrix}1 & 1\\ -1 & 1\end{smallmatrix}\right]$. Thus the PSP divides the time frequency plane into two regions: a region S_0 where (12) is satisfied and the rest of the TF plane $\tilde{S}_0$ where it is not.

Given the stationary phase points $\{(\mu_i,\tau_i)\}_i$, the stationary phase approximation is invoked by replacing (2) by:

$$\hat{x}(t) \quad \approx \quad \frac{1}{C}\Re\left\{\iint_S X_\omega(\tau)h^*_\omega(\tau-t)\,\mathrm{d}\mu\mathrm{d}\tau\right\} \qquad (14)$$

where S is a subset of the TF plane defined as $S = \{\bigcup_i S_i\} \cup \tilde{S}_0$, S_i is the neighbourhood of the ith stationary phase point

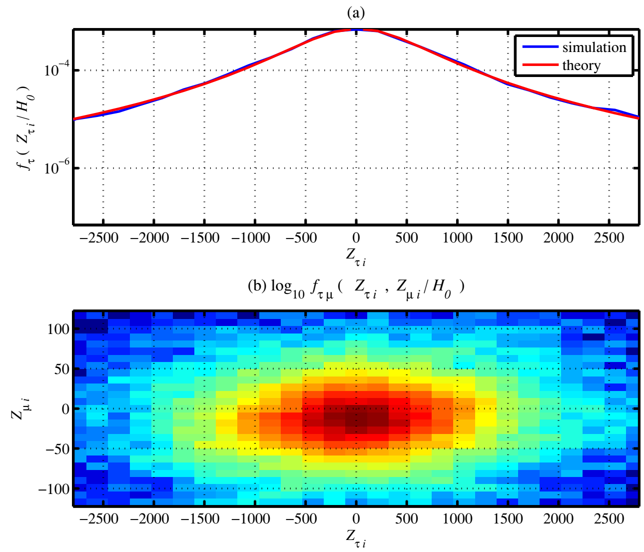

Fig. 1. Null hypothesis, gammatone filter: (a) $f_\tau(Z_{\tau i}|\mathcal{H}_0)$ from simulation in blue and using (16) in red; (b) empirical joint distribution.

such that $(\mu_i, \tau_i) \in S_i$ and $\bigcup_i S_i$ contains all points in the TF plane that satisfy (11). Together the analysis steps of (1), (6) & (7), the selection inequalities (11) & (12) and the synthesis equation (14) form a time-frequency stationary phase approximation (TFSPA).

4. DETECTING STATIONARY PHASE POINTS

Equation (11) is a binary hypothesis test. Under the null hypothesis, $\mathcal{H}_0$, a signal is not present. Under the alternative hypothesis, $\mathcal{H}_1$, a signal that induces a stationary phase point is present. Specifically consider:

$$\begin{aligned}\mathcal{H}_0 : x(t) &= w(t)\\ \mathcal{H}_1 : x(t) &= \mathrm{e}^{\jmath\omega t} + w(t)\end{aligned}$$

where $w(t)$ is zero-mean complex Gaussian white random process with variance σ_w^2. The performance of the test is characterised by the probability of false alarm (type I error), $P_{FA}(||\phi|| < C_1|\mathcal{H}_0)$, and the probability of detection, $P_D(||\phi|| < C_1|\mathcal{H}_1)$. These probabilities can be bounded by

$$P_{FA} \leq \int_{-C_1}^{C_1}\int_{-C_1}^{C_1} f_{\tau,\mu}(Z_{\tau i}, Z_{\mu i}|\mathcal{H}_0)\mathrm{d}Z_{\tau i}\mathrm{d}Z_{\mu i} \quad (15)$$

where $f_{\tau,\mu}(Z_{\tau i}, Z_{\mu i}|\mathcal{H}_0)$ is the joint PDF of $(Z_{\tau i}, Z_{\mu i})$ conditioned on the null hypothesis. Further simplification follows if $Z_{\tau i}$ and $Z_{\mu i}$ are independent in which case the probability can be expressed as products of terms of the form $\int_{-C_1}^{C_1} f_\tau(Z_{\tau i}|\mathcal{H}_0)\mathrm{d}Z_{\tau i}$, where $f_\tau(Z_{\tau i}|\mathcal{H}_0)$ is the PDF of $Z_{\tau i}$ conditioned on $\mathcal{H}_0$.

Under the null hypothesis, $X_\omega(\tau)$, $\frac{\partial}{\partial\omega}X_\omega(\tau)$ and $\frac{\partial}{\partial\tau}X_\omega(\tau)$ are zero-mean complex Gaussian random variables whose variances and cross-correlations can be evaluated using the filter responses $h_\omega(\tau)$, $\frac{\partial}{\partial\omega}h_\omega(\tau)$ and $\frac{\partial}{\partial\tau}h_\omega(\tau)$ and the input noise variance σ_w^2. Equations (8) and (9) appear challenging as they involve ratio's of Gaussian random variables. Fortunately the recent result of [12] addresses this directly. Consider z, which is the ratio of two jointly-Gaussian zero-mean complex random variables a and b with variances σ_a^2 and σ_b^2 respectively and with cross correlation coefficient $\rho = \rho_r + \jmath\rho_i = \frac{E[ab^*]}{\sigma_a\sigma_b}$, where $z = \frac{a}{b} = z_r + \jmath z_i$. In [12] a closed form expression for the PDF of the joint distribution $f_{a/b}(z_r, z_i)$ of z_r and z_i was derived. The PDF of the imaginary part, required here, is developed by integrating over the whole real line, i.e. $f(z_i) = \int_{-\infty}^{\infty} f_{a/b}(z_r, z_i)\mathrm{d}z_r$. Using a standard result for definite integrals from [13] pg. 250, gives

$$f(z_i) = \frac{\frac{\sigma_a^2}{2\sigma_b^2}\{1-|\rho|^2\}}{\left\{\left\{z_i + \frac{\sigma_a}{\sigma_b}\rho_i\right\}^2 + \frac{\sigma_a^2}{\sigma_b^2}\{1-|\rho|^2\}\right\}^{\frac{3}{2}}} \quad (16)$$

This is a symmetrical distribution with a peak at, and hence a mean of, $-\rho_i\frac{\sigma_b}{\sigma_a}$. The spread of the distribution is indicated by $\frac{\sigma_a}{\sigma_b}\sqrt{1-|\rho|^2}$. Further an expression for the CDF, $F(z_i) = \int_{-\infty}^{z_i} f(\lambda)\mathrm{d}\lambda$, can be obtained using [13] pg. 162.

$$F(z_i) = \frac{\frac{1}{2}\left\{z_i + \frac{\sigma_a}{\sigma_b}\rho_i\right\}}{\left\{\left\{z_i + \frac{\sigma_a}{\sigma_b}\rho_i\right\}^2 + \frac{\sigma_a^2}{\sigma_b^2}\{1-|\rho|^2\}\right\}^{\frac{1}{2}}} + \frac{1}{2} \quad (17)$$

Using (16) exact expressions can be obtained for $f_\tau(Z_{\tau i}|\mathcal{H}_0)$ and $f_\mu(Z_{\mu i}|\mathcal{H}_0)$. One such result for the former is illustrated in Fig.1(a). The vertical axis is a logarithmic scale to highlight the non-Gaussian nature of the distribution and the heavy tails. While the pursuit of an analytic expression for the joint distribution $f_{\tau,\mu}(Z_{\tau i}, Z_{\mu i}|\mathcal{H}_0)$ is the subject of ongoing work, experimental evidence such as the empirical distribution of Fig.1(b) strongly suggests that $Z_{\tau i}$ and $Z_{\mu i}$ are independent for Gaussian and gammatone filter banks but not for gammachirp where they are strongly correlated. An approximate theoretical upper bounds on P_{FA} can be obtained by applying the independence assumption to (15) and then using (17) to evaluate each of the two resultant product terms. An example of the result is illustrated in Fig.2 which compares the theoretical result with the false alarm rate measured in simulation for a cochlea-spaced gammatone filter bank [1].

Under $\mathcal{H}_1$, (8) becomes:

$$Z_{\tau i} = \Im\left\{\frac{\jmath\omega + n_\tau(\tau)\mathrm{e}^{-\jmath\omega\tau}}{1 + n(\tau)\mathrm{e}^{-\jmath\omega\tau}}\right\} - \omega$$

where $n(\tau) \sim CN(0, \sigma_n^2)$ is the noise component at the output of the analysis filter $h_\omega(t)$ and $n_\tau(\tau) \sim CN(0, \sigma_\tau^2)$ is

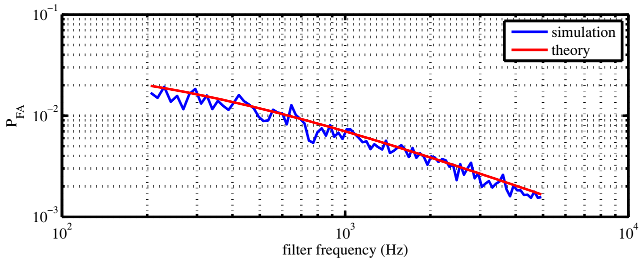

Fig. 2. Probability of false alarm for cochlea-spaced gammatone filter bank with $C_1 = 10$.

the noise component at the output of the time derivative filter $\frac{\partial}{\partial t} h_\omega(t)$. Since $n(\tau)$ and $n_\tau(\tau)$ are the outputs of filters centered ar ω rad/s, the action of the $\mathrm{e}^{-\jmath\omega\tau}$ term is to shift their power spectra to zero rad/s and hence,

$$Z_{\tau i} \quad = \quad \Im\left\{\frac{\jmath\omega + n_\tau(\tau)}{1 + n(\tau)}\right\} - \omega$$

where the noise processes are suitably re-defined. These noise processes are jointly complex Gaussian with correlation coefficient ρ_τ. Assuming that the signal power is much greater than the noise power at the output of analysis filter i.e. $\sigma_n^2 \ll 1$ and $|1 + n(\tau)| \approx 1$ leads to the following approximation

$$Z_{\tau i} \quad \approx \quad \Im\{n_\tau(\tau)\} + \omega\Re\{n(\tau)\} + \Im\{n_\tau(\tau)n^*(\tau)\} \quad (18)$$

While the first 2 terms on the RHS are Gaussian random variables , the third is not. However both the mean $\bar{Z}_{\tau i}$ and the variance $\sigma^2_{Z\tau}$ of $Z_{\tau i}$ in (18) can be evaluated exactly (the latter using Isserlis's theorem [14]) i.e.: $\bar{Z}_{\tau i} = \Im\{\rho_\tau\}\sigma_n\sigma_\tau$ and

$$\sigma^2_{Z\tau} \quad = \quad \frac{\sigma_\tau^2}{2} + \omega^2\frac{\sigma_n^2}{2} - \omega\Im\{\rho_\tau\}\sigma_\tau\sigma_n + \text{smaller terms.}$$

This in turn leads to a Gaussian approximation to the conditional density based on these parameters, i.e.:

$$f_\tau(Z_{\tau i}|\mathcal{H}_1) \quad \approx \quad N(Z_{\tau i}; \bar{Z}_{\tau i}, \sigma^2_{Z\tau}). \quad (19)$$

The quality of this approximation is illustrated in Fig. 3(a). Similar arguments follow for $Z_{\mu i}$ (9) and, as with the null hypothesis, experimental evidence such as Fig. 3(b) suggests that $Z_{\tau i}$ and $Z_{\mu i}$ are independent for Gaussian and gammatone filters.

As well as characterising the performance of (11), the expression presented in this section give insight into developing better detectors. For example, the optimal decision boundary for the binary test is defined as the solution to;

$$f_{\tau,\mu}(Z_{\tau i}, Z_{\mu i}|\mathcal{H}_1) \quad = \quad f_{\tau,\mu}(Z_{\tau i}, Z_{\mu i}|\mathcal{H}_0)$$

Applying the independence assumption leads to separate solutions: (i) $f_\tau(Z_{\tau i}|\mathcal{H}_1) = f_\tau(Z_{\tau i}|\mathcal{H}_0)$ (whose solution can be observed in Fig. 3(a) at the points where the red and black lines intersect); (ii) $f_\mu(Z_{\mu i}|\mathcal{H}_1) = f_\mu(Z_{\mu i}|\mathcal{H}_0)$. While these equations can be be solved numerically, simpler approximations are also of interest for ease of implementation. If, as is evident from Fig. 3(a), the spread of $f_\tau(Z_{\tau i}|\mathcal{H}_0)$ is much larger than the r.m.s. of $f_\tau(Z_{\tau i}|\mathcal{H}_1)$, the former is almost constant over the domain of the latter. It is convenient to approximate $f_\tau(Z_{\tau i}|\mathcal{H}_0)$ with its peak value which is readily obtained from (16). This leads to the following approximation to the optimal decision boundary.

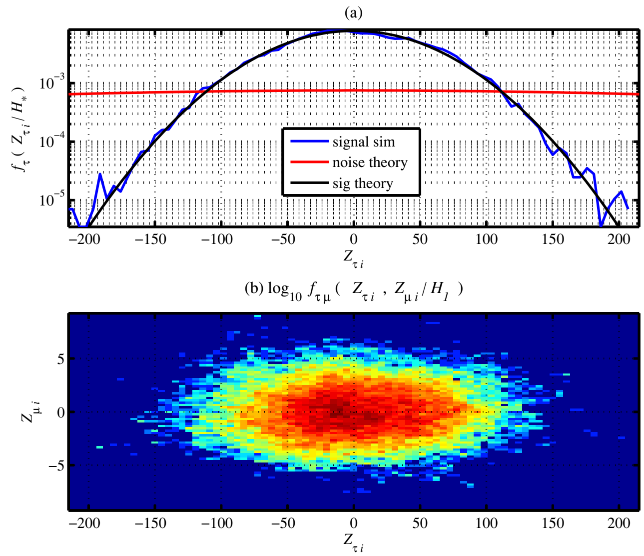

Fig. 3. Alternative hypothesis, gammatone filter, $\sigma_n^2 = -19\,\text{dB}$: (a) $f_\tau(Z_{\tau i}|\mathcal{H}_1)$ simulated in blue; $f_\tau(Z_{\tau i}|\mathcal{H}_1)$ theory (19) in black;$f_\tau(Z_{\tau i}|\mathcal{H}_0)$ theory using (16) in red; (b) empirical joint distribution

$$\{Z_{\tau i} - \bar{Z}_{\tau i}\}^2 \quad = \quad \sigma^2_{Z\tau} \ln\left(\frac{\frac{\sigma_\tau}{\sigma_n}\sqrt{1 - |\rho_\tau|^2}}{\sqrt{\frac{\pi}{2}}\sigma_{Z\tau}}\right)$$

5. CONCLUSIONS

The test for stationary phase points was examined under both the null hypothesis ($\mathcal{H}_0$), where Gaussian noise alone was present, and the alternative hypothesis ($\mathcal{H}_1$), where a constant frequency phasor was added to the noise. For $\mathcal{H}_0$, closed form expressions for the distributions of the individual components of the phase gradient vector were obtained. For gammatone filter banks, empirical evidence suggests that these components are independent of each other and the derived expressions were shown to predict both the non-Gaussian form of the distributions and the false alarm rate. For $\mathcal{H}_1$, the distribution of the individual components were shown to be approximately Gaussian and expressions for the mean and variance were derived to facilitate calculation of the probability of detection. Using expressions from both $\mathcal{H}_0$ and $\mathcal{H}_1$ a simple approximation to the optimal decision boundary was obtained.

6. REFERENCES

[1] B. Mulgrew, "The stationary phase approximation, time-frequency decomposition and auditory processing," *CoRR*, vol. abs/1208.5919, 2012, http://arxiv.org/abs/1208.5919v1, submitted to Trans Signal Processing.

[2] S. Mallat, *A Wavelet Tour of Signal Processing: The Sparse Way*, Academic Press, 3rd edition, 2009.

[3] S. Mandal, S.M. Zhak, and R. Sarpeshkar, "A bio-inspired active radio-frequency silicon cochlea," *Solid-State Circuits, IEEE Journal of*, vol. 44, no. 6, pp. 1814 –1828, jun. 2009.

[4] R. Wong, *Asymptotic Approximations of Integrals*, vol. 34 of *Classics in Applied Mathematics*, Society for Industrial and Applied Mathematics, 2001.

[5] N. Delprat, B. Escudie, P. Guillemain, R. Kronland-Martinet, P. Tchamitchian, and B. Torresani, "Asymptotic wavelet and Gabor analysis: extraction of instantaneous frequencies," *Information Theory, IEEE Transactions on*, vol. 38, no. 2, pp. 644 –664, Mar. 1992.

[6] P. Guillemain and R. Kronland-Martinet, "Characterization of acoustic signals through continuous linear time-frequency representations," *Proceedings of the IEEE*, vol. 84, no. 4, pp. 561 –585, apr 1996.

[7] K. Kodera, R. Gendrin, and C. Villedary, "Analysis of time-varying signals with small BT values," *Acoustics, Speech and Signal Processing, IEEE Transactions on*, vol. 26, no. 1, pp. 64–76, Feb 1978.

[8] Ingrid Daubechies, Jianfeng Lu, and Hau-Tieng Wu, "Synchrosqueezed wavelet transforms: An empirical mode decomposition-like tool," *Applied and Computational Harmonic Analysis*, vol. 30, no. 2, pp. 243 – 261, 2011.

[9] R.F. Lyon, A.G. Katsiamis, and E.M. Drakakis, "History and future of auditory filter models," in *Circuits and Systems (ISCAS), Proceedings of 2010 IEEE International Symposium on*, may. 2010, pp. 3809 –3812.

[10] Toshio Irino and Roy D. Patterson, "A time-domain, level-dependent auditory filter: The gammachirp," *The Journal of the Acoustical Society of America*, vol. 101, no. 1, pp. 412–419, 1997.

[11] F. Auger and P. Flandrin, "Improving the readability of time-frequency and time-scale representations by the reassignment method," *Signal Processing, IEEE Transactions on*, vol. 43, no. 5, pp. 1068–1089, May 1995.

[12] R.J. Baxley, B.T. Walkenhorst, and G. Acosta-Marum, "Complex Gaussian ratio distribution with applications for error rate calculation in fading channels with imperfect CSI," in *Global Telecommunications Conference (GLOBECOM 2010), 2010 IEEE*, dec. 2010, pp. 1 –5.

[13] A. Jeffrey, *Handbook of Mathematical Formulas and Integrals*, Academic Press, 2nd edition, 2000.

[14] L. Isserlis, "On a formula for the product-moment coefficient of any order of a normal frequency distribution in any number of variables," *Biometrika*, vol. 12, no. 1-2, pp. 134–139, 1918.